Front. Optoelectron. China 2008, 1(1–2): 119–122
DOI 10.1007/s12200-008-0020-6

RESEARCH ARTICLE

Wavefront curvature sensor with phase defocus grating

Fengjie XI (✉), Xiaojun XU, Tiezhi WANG, Zongfu JIANG, Yifeng GENG

College of Optoelectronic Science and Engineering, National University of Defense Technology, Changsha 410073, China

Abstract The proposed optimum phase defocus grating for wavefront curvature sensing features an equidistantly quantized two-phase-step and a phase step height of π. The optimum phase defocus grating suppresses the influence of zero-order diffraction. The high diffractive efficiencies of the ± 1 diffraction orders are verified experimentally, showing average values of 38.08% and 40.36% respectively. The phase plate introduces the wavefront deformation, which are measured by wavefront curvature sensing and reconstructed via the Green's Function algorithm. The reconstructed wavefront is compared with the measurement result of a Veeco interferometer. It is verified that the measurement of the self-designed curvature sensor is correct. The error percent of peak-valley value (PV) is 10%, and the error percent of root mean square (RMS) is 2%.

Keywords adaptive optics, wavefront curvature sensor, phase defocus grating, diffractive optics, diffractive efficiency, wavefront measurement

1 Introduction

Increasing applications of adaptive optics, including astronomical observation, high energy lasers, directed energy technique and laser communication, have led to the requirement for a fast, accurate and robust wavefront sensing technique. The promising wavefront curvature sensing technique proposed by Roddier [1] in 1988 requires simultaneous intensity distributions of two defocused spots as input. The wavefront curvature sensor in astronomical adaptive optics with a vibrating membrane mirror can easily change the defocus distance, which is indispensable to atmospheric conditions and extended sources. However, disadvantages such as complexity, pseudo-simultaneous measurement, and an unstable system [2], can be barriers for spreading wavefront curvature sensing in the optical metrology, laser-related and other adaptive optics fields.

Recently, the wavefront curvature sensor has been implemented with a defocus grating [3,4]. The defocused spots are recorded as physically separated images on a single camera, which eliminates the need for complex optics or for the synchronization of multiple cameras. The wavefront curvature sensor with a defocus grating is a powerful technique with applications in many fields. Nevertheless, a diffraction grating is chromatic and the defocus distance is fixed. Some researchers are contributing to overcome these disadvantages [5].

The detector plane in the wavefront curvature sensor with a grating is both the focus plane in the zero diffraction order and the defocus planes in the ± 1 orders. When an amplitude defocus grating is used in close proximity to a lens, as in Refs. [3] and [4], the spot of the zero-order is much brighter than that of the ± 1 orders, which easily makes the detector reach saturation. The far more serious problem is limited light available in ± 1 orders. Zero-order diffractive efficiency must be suppressed to increase the light available and eliminate saturation of the detector. The wavefront curvature and the wavefront itself are obtained by measuring the normalized difference of intensity distributions of two defocus spots, thereby making diffractive efficiencies in the ± 1 diffraction orders equal. Binary phase grating can modify the distribution of diffractive efficiencies in various orders. The diffractive efficiency of phase defocus grating used in the wavefront curvature sensor must be specially considered.

The wavefront curvature sensor with the phase defocus grating is fabricated. The absolute diffractive efficiencies of the 0, ± 1 diffraction orders were measured experimentally. The wavefront deformation was introduced by the phase plate, which was measured by wavefront curvature sensing and reconstructed via the Green's Function algorithm. The reconstructed wavefront is compared with the measurement result of a Veeco interferometer.

Translated from *Acta Optica Sinica*, 2007, 27(2): 377–378 [译自: 光学学报]

E-mail: xifengjie@163.com

2 Phase defocus grating

The defocus grating is an off-axis Fresnel-zone plate, thus the analysis of the diffractive efficiency is similar to the classical Fresnel-zone plate. The transfer function of the continuous phase profile Fresnel-zone plate should be written as

$$t(\xi) = \exp(\mathrm{i}2\pi([\xi] + 1 - \xi), \tag{1}$$

where $\xi = r^2/P^2$, r is the radial coordinate of the Fresnel-zone plate, $P^2 = 2\lambda f$ is the radius of the first Fresnel-zone, λ is the wavelength, f is the effective focal length of the Fresnel-zone plate, the operator $[n]$ indicates the integer part of number n, and the modulo of the Fresnel-zone plate in this paper is 2π. The continuous phase profile can be quantized into discrete phase levels. After analyzing the diffractive efficiency, the continuous phase profile and binary multi-phase-step relief Fresnel-zone plate blazes in the +1 diffractive order, such that it cannot fulfill the requirement of equal diffractive efficiencies in the ± 1 diffractive orders [6]. When $L = 2$, the diffractive efficiencies are equal in the ± 1 diffraction orders. Therefore, the wavefront curvature sensor can be implemented with an off-axis binary phase Fresnel-zone plate [7].

On assumption that the phase-step height is $S\pi$ and phase-step width is w, where $0 \leqslant \mathrm{S} < 2$, $0 \leqslant w < 1$, the transfer function can be expressed as

$$t(\xi) = \exp(\mathrm{i}\pi S)\mathrm{rect}\left(\frac{\xi}{w}\right) \cdot \sum_{n=0}^{N-1} \delta\left[\xi - \left(n + \frac{w}{2}\right)\right] + \mathrm{rect}\left(\frac{\xi}{1-w}\right) \cdot \sum_{n=0}^{N-1} \delta\left[\xi - \left(n + \frac{1+w}{2}\right)\right], \tag{2}$$

N is the total number of the Fresnel-zones. The diffractive efficiency in the zero order is given by

$$\eta_0 = |\cos(S\pi)w + 1 - w + \mathrm{i}\sin(S\pi)|^2. \tag{3}$$

To be as simple as possible, diffractive efficiency in other diffractive orders is given by

$$\eta_m = \frac{4\sin^2(\pi S/2)\sin^2(\pi m w)}{\pi^2 m^2}. \tag{4}$$

It can be seen from Eq. (4) that the ± 1 order diffractive efficiencies are equal, regardless of varying phase-step height and width. As can be seen from Eqs. (3) and (4), when $w = 1/2$, $S = 1$, i.e., with an equidistantly quantized binary phase step and phase height of π, the diffractive efficiency η_0 of the zero-order reaches the minimum, $\eta_0 = 0$. At the same time, the diffractive efficiencies $\eta_{\pm 1}$ of the ± 1 orders reach the maximum, $\eta_{\pm 1} = (4/\pi^2) \approx 40.5\%$. If the phase-step height deviates from 1, or the phase-step width deviates from 1/2, the zero-order diffractive efficiency will increase gradually up to 1 and the zero-order diffractive efficiency will decrease gradually to 0.

The defocus grating employed in the wavefront curvature sensor is an off-axis binary phase Fresnel-zone plate. The various diffraction orders of the defocus grating correspond to the convergent or divergent spherical wave with the foci out of the axis. The +1 order diffractive light ($m = -1$) is the convergent spherical wave with the wave vector (kx_0/f,0,k_z), which is focused at point (x_0,0,f), where x_0 is the off-axis distance.

Accordingly, the equidistantly quantized binary phase-step defocus grating, with phase height of π, can be employed in the wavefront curvature sensor to eliminate the saturation of the zero-order diffractive light and equalize the ± 1 order diffractive efficiencies.

In practice, defocus grating is combined with a short focal length lens. A photoelectric detector, such as a CCD camera, is located on the focal plane of the lens. The combination forms a focused spot in the zero order and two defocused spots in the ± 1 orders. The two defocused spots correspond to two intensity distributions that the wavefront curvature sensor requires. Consequently, the wavefront curvature sensor is all-optical implemented with a defocus grating.

3 Experimental verifications

The equidistantly quantized binary phase defocus grating is fabricated in the laboratory; it is designed for a wavelength of 632.8 nm, with aperture of 28 mm and phase-step height of π. The phase grating is shaped on a fused SiO_2 base. The effective focal length of the defocus grating is 3600 mm, with an off-axis distance of 37.5 mm. The focal length of the lens combined with the defocus grating is 105 mm. With the illumination of an expanded He–Ne (632.8 nm) laser beam, the spot distributions are detected with a linear CCD camera on the focal plane of the lens. The linear CCD camera is a CV-A10 CL model BW 10 bits production from the JAI Co. The CCD camera has 782×582 square pixels, which is 8.37 μm × 8.37 μm, with the background grey value of 100 and the signal-to-noise ratio is larger than 55 dB.

The diffracted spots sampled with this CCD camera are shown in Fig. 1. The left one is the +1 order spot, the middle is the zero order spot, and on the right is the -1 order spot. The spots in other orders are outside the detector plate of the CCD camera. Substituting a plain fused SiO_2 base for phase grating, the defocus spot representing the total energy is recorded (Fig. 2). The absolute diffractive efficiencies are measured with the analysis of the spots' grey values. After measuring and averaging 10 times, the average diffractive efficiencies in

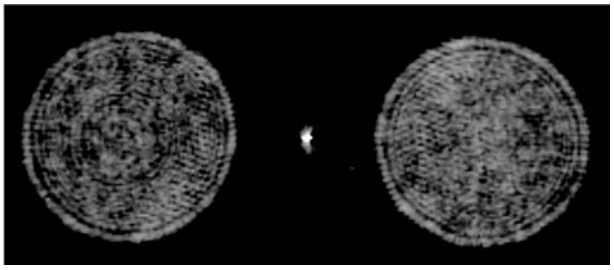

Fig. 1 Spots in 0, ± 1 diffractive order of defocus grating

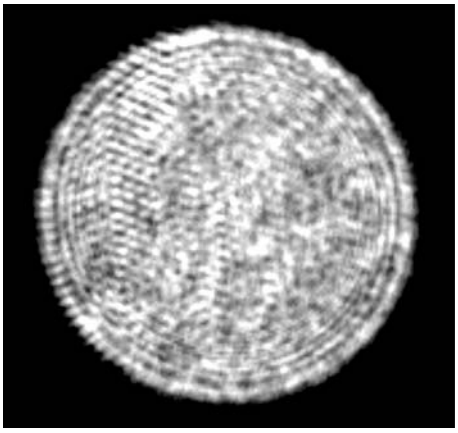

Fig. 2 Defocus spot representing total energy without phase grating

the 0, ± 1 orders are obtained and listed in Table 1. The average diffractive efficiencies in the ± 1 orders are 38.08% and 40.36% respectively, which are slightly lower than the theoretical value of 40.5%. The average diffractive efficiency in the 0 order is 0.75%. The percent repeatability error of the measurement is $\pm 2\%$.

Table 1 Absolute diffractive efficiency in 0, ± 1 orders

	+1 order	0 order	−1 order
diffractive efficiency/%	38.08	0.75	40.36

It can be seen from Fig. 1 and Table 1 that the equidistantly quantized, binary phase-step defocus grating, at phase height of π, can suppress diffractive efficiency in the zero order to eliminate saturation of the detector and equalize diffractive efficiencies in the ± 1 orders. The diffractive efficiencies in the 0, ± 1 orders of the defocus grating are affected by the fabrication technique, such as accuracy of the phase-step height and phase-step width, and smoothness and steepness of the phase-step. Qualitatively, the zero-order spot appears and diffractive efficiencies in the ± 1 orders are slightly lower than the theoretical value because phase-step height is not precisely π and the phase-step is not exactly equidistantly quantized. The diffractive efficiency in the +1 order and that in the -1 order are different because steepness of the phase-step is not perfectly vertical — a condition which can be corrected in software.

An expanded, unpolarized He–Ne laser probe beam (632.8 nm) passing through the phase plate is detected by the wavefront curvature sensor. The plate was measured by the Veeco interferometer, and majority of the aberration is the defocus and astigmatism. The intensity distribution of the two defocused spots recorded by the CCD is exhibited in Fig. 3.

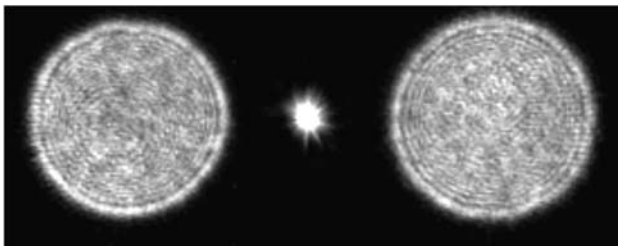

Fig. 3 Two experimental defocused images with aberration of phase plate

Curvature signal, which is the signal of the intensity derivate, and contour plot, which is the phase map of the phase plate measured with the curvature sensor constructed via Green Function algorithm [8], are represented in Fig. 4. The constructed aberration models are consistent with the interference measurement. The curvature sensor and Veeco interferometer measurements are listed in Table 2, with the peak-valley value error of 10% and root-mean square of 2%.

4 Conclusions

It is shown that phase defocus grating, which has the properties of equidistantly quantized, binary phase-step defocus grating, and phase height of π, is the optimum choice for the wavefront curvature sensor. The equidistantly quantized binary phase defocus grating is fabricated, and the high diffractive efficiencies are measured experimentally. The diffractive efficiencies in the ± 1 orders are 38.08% and 40.36% respectively. The sources of the errors, such as limits of the fabrication technique, are described qualitatively. The aberration wavefront is measured with the wavefront curvature sensor and reconstructed via the Green Function algorithm. The measurement of the sensor with a phase defocus grating is correct compared with that of the Veeco interferometer. There exists an error of 10% in peak-valley value as well as an error of 2% root-mean square.

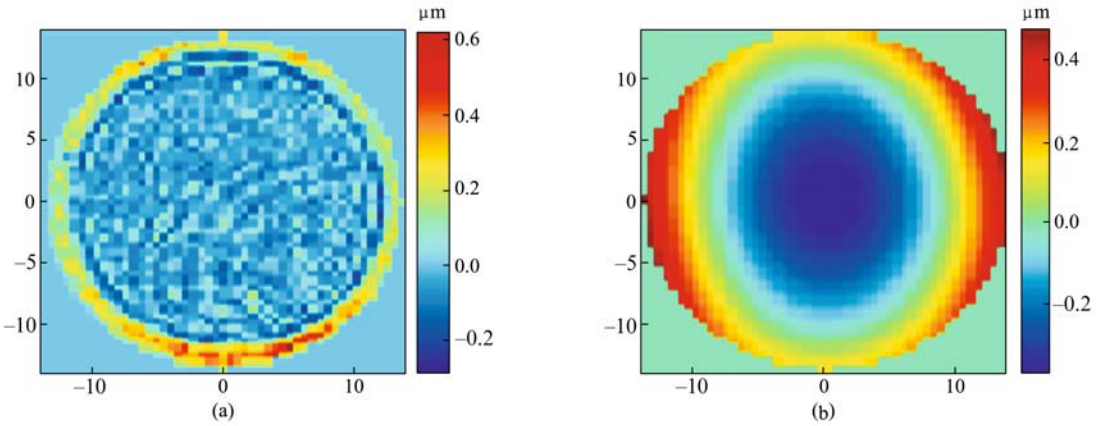

Fig. 4 Intensity derivate signal and phase map of phase plate. (a) Curvature signal, radius = 14 mm, wavelength = 0.6328 μm; (b) contour plot, PV = 0.8412 μm, RMS = 0.1798 μm

Table 2 Comparison of curvature sensor and Veeco measurement

unit	peak-valley value	root-mean square
Veeco interferometer/μm	0.762	0.176
curvature sensor/μm	0.8412	0.1798
error percent/%	10	2

References

1. Roddier F. Curvature sensing and compensation: a new concept in adaptive optics. Applied Optics, 1988, 27(7): 1223–1225
2. Forbes F F, Roddier N A. Adaptive optics using curvature sensing. Proceedings of SPIE, 1991, 1542: 140–147
3. Blanchard P M, Greenaway A H. Simultaneous multiplane imaging with a distorted diffraction grating. Applied Optics, 1999, 38(32): 6692–6699
4. Blanchard P M, Fisher D J, Woods S C, et al. Phase-diversity wave-front sensing with a distorted diffraction grating. Applied Optics, 2000, 39(35): 6649–6655
5. Blanchard P M, Greenaway A H. Broadband simultaneous multiplane imaging. Optics Communications, 2000, 183(1–4): 29–36
6. Swanson G J, Veldkamp W B. Diffractive optical elements for use in infrared systems. Optical Engineering, 1989, 28(6): 605–608
7. Xi F J, Jiang Z F, Xu X J, et al. High-diffractive-efficiency defocus grating for wavefront curvature sensing. Journal of the Optical Society of America A, 2007, 24(11): 3444–3448
8. Woods S C, Greenaway A H. Wave-front sensing by use of a Green's function solution to the intensity transport equation. Journal of the Optical Society of America A, 2003, 20(3): 508–512